Desalination and Water Treatment
www.deswater.com
doi: 10.5004/dwt.2022.28306

253 (2022) 231–238
March

A new photocatalytic reactor for hexachlorobenzene removal in water

Yulin Jiang*, Jianfu Zhao

State Key Laboratory of Pollution Control and Resources Reuse, College of Environmental Science and Engineering, Tongji University, Shanghai 200092, China, Tel: 86 21 65981831; emails: yljiang82@126.com (Y. Jiang), zhaojianfu@tongji.edu.cn (J. Zhao)

Received 24 March 2020; Accepted 16 February 2022

ABSTRACT

A new photocatalytic reactor with a thin-film TiO_2 catalyst attached on the inner wall of quartz glass pipes under UV light radiation was assembled and applied for the removal of hexachlorobenzene (HCB) in water. The results indicated that the degradation effect of HCB was higher in the UV/photocatalytic system at lower flow velocities owing to the longer residence time. As the UV light intensity increased, the degradation efficiency of HCB was enhanced correspondingly. Moreover, an enhancement on the removal effect of HCB was observed with the addition of humic acid. It should be noted that the improvement extent of HCB removal rate was much higher at low humic acid concentration compared to that at higher humic acid concentration. The phenomenon can be ascribed to the photosensitization in the presence of suitable amount of humic acid in the photoreaction system. To further describe these effects, a mathematical model was developed and then verified with experimental data, which validated the predictive capability and demonstrated the removal ratio in terms of initial HCB concentration and UV light intensity.

Keywords: Drinking water treatment; Hexachlorobenzene; UV; TiO_2 film; Photocatalytic oxidation; Humic acid; Mathematical model

1. Introduction

Hexachlorobenzene (HCB) is a kind of hazardous and persistent toxic pollutant previously used as a fungicide, and has been banned globally by the Stockholm Convention on Persistent Organic Pollutants [1,2]. Although the production and utilization of HCB has ceased in the last century, the compound is still generated inadvertently in many countries as a byproduct of manufacturing of various chlorinated compounds such as pesticides [3]. HCB can be found in aquatic systems from industrial discharge and surface runoff close to the sites of production and/or disposal. Several studies reported that 311.7 ng L^{-1} HCB was found in natural water in Brazil [4] and 12.2 μg g^{-1} dry weight HCB was detected in river sediments surrounding PCP-producing factories in China [5]. Although the detected concentration of these substances in natural waters is generally low, it is bioaccumulative and harmful to humans and the environment, since it is considered a carcinogen [6,7]. The level of HCB is also regarded as one of the non-regular indices in the newly issued drinking water standard in China [8].

Slightly soluble hazardous materials can hardly be removed by conventional water treatment processes [9]. Several methods have been able to remove persistent organic pollutants (POPs) from water including membrane filtration [10] and adsorbents [11]. However, these methods only transfer pollutants from one phase to another, rather than chemically destroying the toxic compound. Fenton-based processes have been reported to effectively remove POPs in soil and water [12–14], but the optimal pH for the Fenton process is typically between 3.0 and 4.0, which provides a big constraint for drinking water treatment.

Titanium dioxide (TiO_2) is a semiconductor that has been frequently used as a photocatalyst for environmental and energy applications including water treatment [15].

* Corresponding author.

Conventional TiO_2 can undergo photoexcitation under UV-irradiation and generate an electron-hole pair with a high redox potential that will enable the degradation of aqueous organic compounds, particularly at ambient temperature and pressure conditions [16]. Many research efforts have been focused on the practical application of TiO_2 in the water treatment system. Initially, TiO_2 powder was directly used as a photocatalyst to remove pollutants in water [17], but the need of a post-treatment to separate the TiO_2 slurry from the treated solution is not considered cost-effective [18,19]. Recently, depositing TiO_2 films on different types of substrates has been tested in order to substitute the need of an additional unit operation in the treatment plant. For example, glass beads [20] or rings [21], cotton materials [22], perlite granules [23], quartz [24], porous aluminum foil [25], stainless steel [26], glass tubes [27], and pumice stones [28] have been used as substrate for the immobilization of this photocatalyst. These studies have shown that immobilizing TiO_2 on substrates is effective for the degradation of many pollutants including pesticides, pharmaceuticals, and dyes [29–33]. From these studies, two main factors can be directly correlated to the degradation efficiency of pollutants: one is the photocatalyst specific surface area and the other is the UV light intensity.

In this study, the specific objectives included: (1) to develop a novel and tubular reactor with immobilized TiO_2 in glass that can be operated continuously for long reaction time; (2) to investigate the kinetics and impact factors of the degradation effect of HCB in the photoreaction system; (3) to establish a mathematical model to validate the predictive capability and demonstrated the removal ratio in terms of initial HCB concentration and UV light intensity.

2. Experimental

2.1. Materials and methods

All the chemicals were at least ACS grade and purchased from Sinopharm Chemical Reagent Co., Ltd. The synthesis of the TiO_2 photocatalyst was done by employing the sol-gel method [34]. Titanium tetra-butoxide (97% purity) was used as the precursor material. Calculated quantity of titanium butoxide was dissolved in inisopropyl alcohol (IPA) under intense stirring. HNO_3 as the catalyst was added drop wise to increase the rate of reaction. The molar ratio of titanium tetra-butoxide to water was 1:1. Then, deionizing water (1.5 mL) have been added drop wise for hydrolysis of the sol. The solution had a transparent yellowish tinge and was kept for 24 h at room temperature until film deposition. The raw water was prepared with distilled water spiked with calculated amount of HCB standard sample.

2.2. Determination of hexachlorobenzene

The photodegradation of HCB was monitored using a gas chromatographer (Shimadzu GC-2010) with a HP-5 fused silica capillary column (30 m × 0.32 mm I.D., film thickness of 0.25 μm). Residual concentrations of HCB in water were extracted with n-hexane, and one microliter of the extraction was analyzed in the GC apparatus. The analyses were carried out under the following conditions: injector temperature, 250°C; detector temperature, 290°C. The temperature of the GC oven was programmed as follows: 100°C, isothermal for 2 min, then the temperature was raised at 10°C/min to 250°C and held at 250°C for 4 min. N_2 was the carrier gas at a flow rate of 3.0 mL/min.

2.3. Reactor set-up and procedure

The averaged UV irradiance in this study was determined by using KI/KIO_3 actinometer method proposed by Bolton et al. [35] based on the following photochemical reaction (1).

$$8I^- + IO_3^- + 3H_2O + h\nu \rightarrow 3I_3^- + 6OH^- \quad (1)$$

The actinometer solution was composed of 0.6 M potassium iodide (KI) and 0.1 M potassium iodate (KIO_3) in a 0.01 M sodium tetraborate ($Na_2B_4O_7$) buffer solution. The concentration of photoproduct (triiodide complex, I_3^-) can be accurately quantified using its maximum spectral absorption at 352 nm without being interfered by other components in the actinometer solution. The quantum yield of I_3^- (Φ) at different wavelengths was calculated using the linear equation developed in a prior study ($\Phi = 3.558–0.0113\ \lambda$) [36].

The following Eqs. (2)–(6) illustrate the procedures of irradiance measurements:

$$\left[I_3^-\right](M) = \frac{A_{352}(\text{sample}) - A_{352}(\text{blank})}{\varepsilon\left(M^{-1}cm^{-1}\right)} \quad (2)$$

$$\text{moles } I_3^- = \left[I_3^-\right] \times V(L) \quad (3)$$

$$\text{Einsteins (moles of photons)} = \frac{\text{moles } I_3^-}{\phi(\text{mol / einsteins})} \quad (4)$$

$$\text{Photon irradiance}\left(E_p, \text{einstein } s^{-1}cm^{-2}\right) = \frac{\text{einsteins}}{\text{area}\left(cm^2\right) \times \text{time}(s)} \quad (5)$$

$$\text{irradiance}\left(E, Wcm^{-2}\right) = E_p \times \text{photonenergy} = E_p \times h\nu_\lambda N_A \quad (6)$$

where A_{352} (sample) and A_{352} (blank) are the absorbance of sample and blank solutions at 352 nm (cm^{-1}), respectively, at specific exposure time; ε is the molar absorption coefficient of I_3^- (27,636 $M^{-1}\ cm^{-1}$); V is the total irradiated volume of the sample solution (L); h is the Planck constant (6.626×10^{-34} J s); ν_λ is the wave frequency (s^{-1}); N_A is the Avogadro constant ($6.022 \times 10^{23}\ mol^{-1}$).

2.4. Reactor set-up and procedure

The experimental unit was composed of a raw water tank, pressure stabilizing tank, and photoreactor, as shown in Fig. 1. The pressure stabilizing tank was used to keep the flow uniform. The photoreactor was composed of 30 quartz

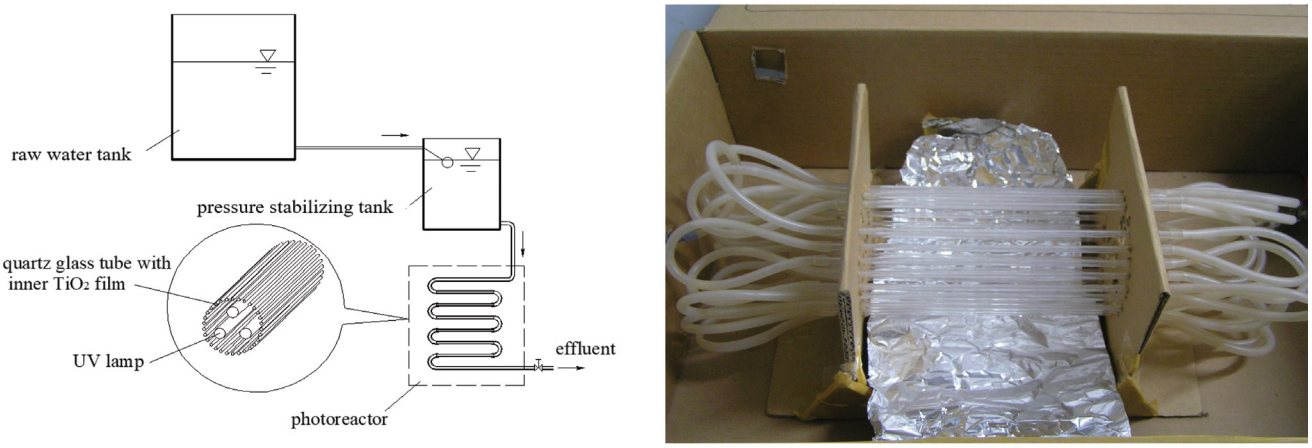

Fig. 1. Schematic diagram of the reactor set-up designed to photocatalytically assess the catalyst supported in the quartz glass tubes.

glass tubes with UV lamps inside each tube. The inside diameter of the tubes was 3 mm, and they were placed in a circle, joined in line with short silicone tubes. The TiO_2 was supported on the inner wall of the tubes by a repeated dip-coating method, air drying and calcination at 400°C for 10 min. When the coating process was completed and the tubes were sufficiently cooled, they were washed in distilled water assisted by air bubbling in a vessel for a few minutes in order to remove the titanium that was not properly attached to the tubes. A control valve was mounted on the effluent pipe to regulate the flow rate. The UV light intensity was adjusted by changing the number of UV lamps. The wavelength of the lamps was 254 nm and the relationship between UV light intensity and the number of the lamps is shown in Table 2.

3. Results and discussion

3.1. Effect of HCB concentration

Different initial concentrations of HCB in water were treated in the photoreactor under the same UV light intensity of 80 μW/cm². Fig. 2 shows the effluent concentration of HCB at different flow rates for each initial HCB concentration tested. The experimental data were linearly fit and the corresponding fitting equations are shown in Table 1. According to Fig. 2 and Table 1, the HCB concentration in the effluent increased with the variation of the flow velocity when the flow velocity ranged from 0.03 to 0.16 m/s. Specifically, the degradation efficiency of HCB deteriorated along with the increase of the flow velocity. The phenomenon can be attributed to the higher residence time at lower flow velocities that allowed relatively more complete degradation of HCB in the UV/photocatalytic system [37]. To be noted, the degradation efficiency of HCB almost stayed the same regardless of the initial concentration level of HCB, which demonstrated that the initial concentration of HCB had little influence on the degradation effect of HCB when applying the photoreactor system.

The degradation effect of HCB at very low flow velocities was further investigated. As depicted in Fig. 2, when the initial concentration was at 51.6 μg/L and the flow velocity was less than 0.025 m/s, the HCB concentration in the effluent rose. The diffusion of the solute in water was mainly caused by two factors including the concentration gradient and turbulent diffusion [38]. When the water was in a relatively static state, the effect of turbulent diffusion tended to be negligible. Therefore, the low turbulence intensity and the small transmission capacity of such low HCB concentration failed to offer effective diffusion to promote degradation.

Table 1
Fitting equations at different initial concentrations under the UV intensity of 80 μW/cm² (flow velocity > 0.02 m/s)

Initial HCB concentration	Fitting equation
C_0 = 23.5 μg/L	$y = 163.92x + 0.66$ $R^2 = 0.959$
C_0 = 37.0 μg/L	$y = 168.35x + 9.71$ $R^2 = 0.996$
C_0 = 51.6 μg/L	$y = 188.15x + 27.41$ $R^2 = 0.906$
C_0 = 240.0 μg/L	$y = 168.54x + 9.62$ $R^2 = 0.996$

3.2. Effect of UV light intensity

UV light intensity is a critical factor in the degradation effect of HCB. To explore the effect of ultraviolet light intensity on the degradation of HCB, the intensity of UV radiation in the photoreaction system was adjusted by changing the number of UV lamps. Table 2 lists the corresponding relationship between the number of lamps and the UV light intensity. The degradation effect of HCB at the initial concentration of 240 μg/L under different UV intensities are shown in Fig. 3. When increasing the UV light intensity, the degradation effect of HCB was enhanced obviously. The experimental data were linearly fit and the corresponding fitting equations are shown in Table 3. Therefore, the effect of removing HCB can be greatly improved by enhancing the intensity of UV radiation [39]. Moreover, the degradation efficiency of HCB was on the decline with the increase of flow velocity even at a much higher initial HCB concentration of 240 μg/L, which was consistent with the results in Fig. 2.

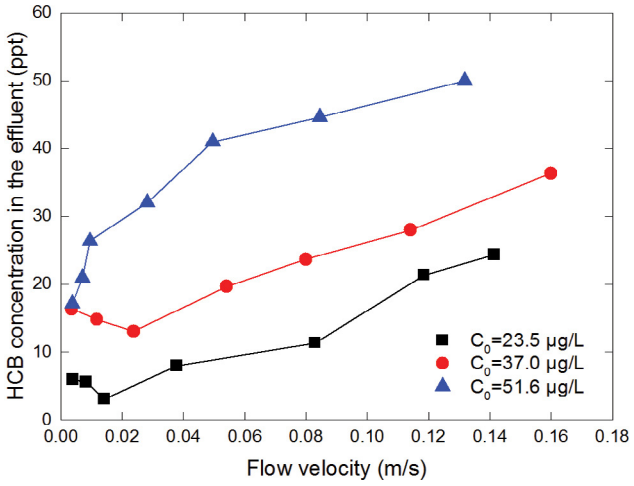

Fig. 2. Degradation effect of HCB at different initial concentrations under the same UV light intensity of 80 μW/cm².

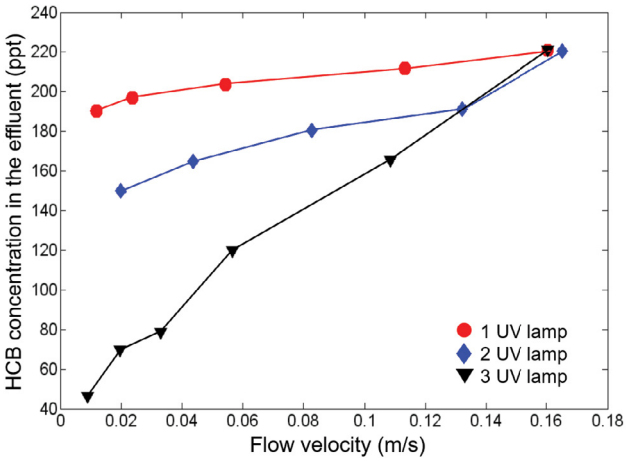

Fig. 3. The degradation effect of HCB at the initial concentration of 240.0 μg/L under different UV intensities.

Table 2
Number of UV lamps and their intensities

Number of lamps	1	2	3
UV light intensity (μW/cm²)	80	161	243

Table 3
Fitting equations at the initial HCB concentration of 240 μg/L under different UV intensities

UV lamps	Fitting equations
1	$y = 190.16x + 190.93$ $R^2 = 0.968$
2	$y = 434.29x + 142.97$ $R^2 = 0.955$
3	$y = 1117.10x + 44.77$ $R^2 = 0.989$

3.3. Effect of other organic matter

In actual water body, the existence of organic matter in water may have an impact on the degradation rate of HCB. To investigate the effect of organic matter, humic acid as a model compound was added into the photoreaction system. The experiment was conducted at the initial HCB concentration of 240 μg/L in raw water under the UV light intensity of 80 μW/cm² with the water flow velocity kept at 0.15 m/s. Different amounts of humic acid were added to the raw water and the amount was expressed by COD_{Mn}. As shown in Fig. 4, the HCB concentration in the effluent decreased with the addition of humic acid. Particularly, the removal rate of HCB at the humic acid concentration of 2.0 mg/L COD_{Mn} achieved 63.6%. When further adding humic acid to 4.2 mg/L COD_{Mn}, the removal rate increased only 18.2%. Humic acid can play a double role as photosensitizer and inhibitor. Hence, suitable amount of humic acid can facilitate the degradation of HCB. However, the humic acid can compete with the degradation of the target contaminant with the increase of humic acid, which resulted in the reduction of the improvement of the photodegradation efficiency of HCB [40]. Overall, the addition of humic acid can enhance the removal efficiency of HCB in the photoreaction system.

3.4. Reaction model

The internal structure of the quartz glass tubes is shown in Fig. 5 with a 2-D coordinate system. There is a thin TiO_2 film inside the tube and the thickness of the film is $(x_2–x_1)$ mm. The UV light is positioned vertical to the tube and I_0 is its initial intensity. The UV intensity and pollutant concentration in the body water are I and S_b, respectively. The HCB concentration on the surface of the TiO_2 film is q_w. S_w is HCB concentration in the water film near the surface, and q is the HCB concentration adsorbed in the TiO_2 film.

In order to establish a kinetic model for the photoreactor, some premises are put forward as follows: (1) the UV lamp is a linear light source and the intensity is equal around the lamp; (2) the thickness of the TiO_2 film loaded on the quartz glass tube is uniform; and (3) the concentration of the pollutant in the water is uniform. According to the mass-balance principle in an ideal plug flow reactor operated in a steady state, the reaction equation in a differential element volume is shown as Eq. (7):

$$\frac{\pi d^2}{4}dy\frac{dS_b}{dt} = \frac{\pi d^2}{4}vS_b - \frac{\pi d^2}{4}v\left(S_b + dS_b\right) + \mu\left(S_b\right)\frac{\pi d^2}{4}dy \tag{7}$$

where y represents the total length of the quartz glass tubes and v is the internal flow velocity; d represents the inside diameter of the tubes; S_b represents the HCB concentration at the point y of the total length of the quartz glass tubes, and $\mu(S_b)$ is the degradation rate of the pollutant.

During steady-state conditions, the pollutant concentration at a section does not change over time. That is to say, $dS_b/dt = 0$; thus, Eq. (7) can be simplified as follows:

$$v\frac{dS_b}{dy} = \mu\left(S_b\right) \tag{8}$$

During the TiO_2 photocatalytic reaction in a specific reactor, the degradation rate is related to the UV intensity, initial pollutant concentration, and some interfering substances in the water [41], which can be expressed as Eq. (9):

$$\mu\left(S_b\right) = -k_1 I^{\alpha} q^{\beta} + \sum_{i=1}^{n} \mu\left(c_i\right) \tag{9}$$

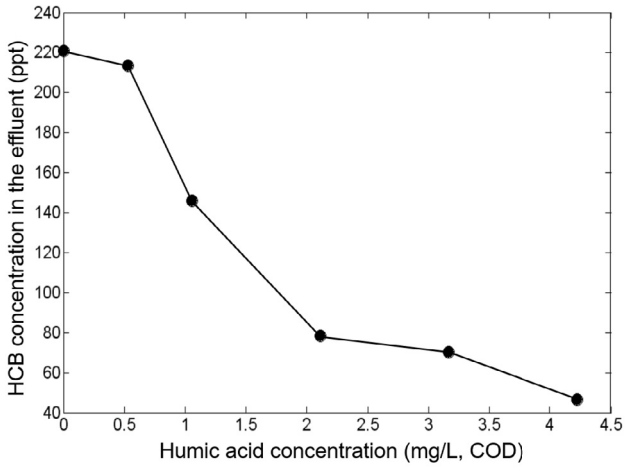

Fig. 4. The effect of humic acid on the removal of HCB. (Experimental conditions: initial HCB concentration = 240.0 μg/L, UV light intensity = 80 μW/cm², water flow velocity = 0.15 m/s).

where $\mu(S_b)$ is the degradation rate of the pollutant; I represents the UV intensity in the TiO_2 film, W/cm²; q is the pollutant concentration in the TiO_2 film, mg/g; $\mu(c_i)$ is the effect of substance i on the degradation rate; and α and β are the reaction orders.

The attenuation of the UV intensity in the photocatalyst film relates to the character of the photocatalyst and the wavelength of the UV lamp [41]. Therefore, the relation can be expressed by Eq. (10):

$$I = I_0 \times 10^{-\gamma\left(x_2 - x\right)} \quad x_1 < x < x_2 \tag{10}$$

where I_0 is the initial UV intensity, W/cm²; and γ represents the attenuation coefficient of the UV intensity in the TiO_2 film. It can be assumed that $\bar{I}$ is the average UV intensity and Eq. (10) can be integrated into Eq. (11) as follows:

$$\bar{I} = \int_{x_1}^{x_2} \frac{I_0 \times 10^{-\gamma\left(x_2 - x\right)}}{x_2 - x_1} d_x = \frac{\left(1 - 10^{-\gamma\left(x_2 - x_1\right)}\right) I_0}{\gamma \ln 10 \left(x_2 - x_1\right)} = k_2 I_0 \quad x_1 < x < x_2 \tag{11}$$

In general, the adsorption of pollutants by photocatalysts have a Langmuirian isotherm nature [42]; therefore, the pollutant concentration q_w on the TiO_2 surface is as follows:

$$q_w = \frac{q_{\max} b S_w}{1 + b S_w} \tag{12}$$

where b represents the Langmuir–Hinshelwood adsorption constant, L/mg; $q_{\max}$ is the maximum adsorption ability, mg/g;

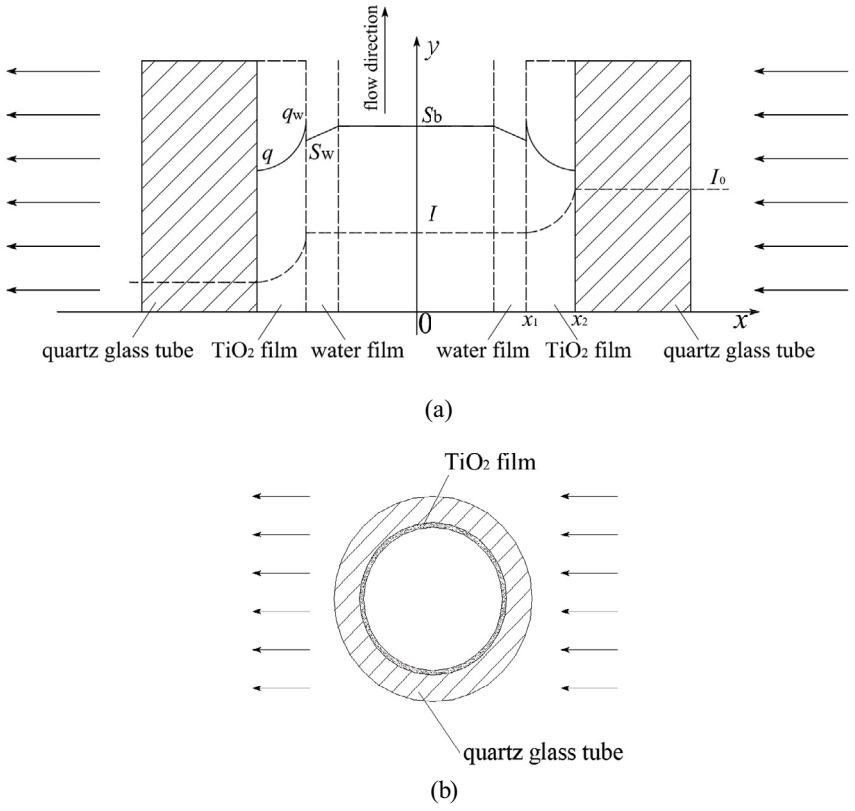

Fig. 5. The structure of the quartz glass tube with TiO_2 inside (a) profile and (b) sectional view.

and S_w is the concentration of pollutant in the water film near the photocatalyst, mg/L. If the mass transfer coefficient of the pollutant in the water film is defined as k_3, then the relation between S_w and S_b can be expressed as Eq. (13):

$$S_w = k_3 S_b \tag{13}$$

When the pollutant concentration is very low, the value of bS_w is far less than 1, and Eq. (12) can be modified as:

$$q_w = q_{\max} bS_w = k_3 q_{\max} bS_b \tag{14}$$

The transformation of the pollutant in the TiO_2 film can be described in Eq. (15):

$$q = k_4 q_w = k_4 k_3 q_{\max} bS_b \tag{15}$$

Eqs. (8), (9), (11) and (15) can be integrated into Eq. (16):

$$v\frac{dS_b}{dy} = -k_1\left(k_2 I_0\right)^{\alpha}\left(k_4 k_3 q_{\max} bS_b\right)^{\beta} + \sum_{i=1}^{n}\mu\left(c_i\right) = -k_1 k_2^{\alpha} k_3^{\beta} k_4^{\beta} q_{\max}^{\beta} b^{\beta} I_0^{\alpha} S_b^{\beta} + \sum_{i=1}^{n}\mu\left(c_i\right) \tag{16}$$

If there is no other substance affecting the reaction, then the value of $\sum_{i=1}^{n}\mu\left(C_i\right)$ is 0. By integrating along the tube, Eq. (17) is obtained and rewritten as Eq. (18):

$$v\left(S_{b0} - S_{bi}\right) = \frac{-\delta I_0^{\alpha}}{\beta+1}\left(S_{b0}^{\beta+1} - S_{bi}^{\beta+1}\right) \tag{17}$$

$$\frac{1-\eta^{\beta+1}}{1-\eta} = -\frac{\left(\beta+1\right)v}{S_{\mathrm{bi}}^{\beta}\delta I_0^{\alpha}} \tag{18}$$

where $\delta = k_1 k_2^{\alpha} k_3^{\beta} k_4^{\beta} q_{\max}^{\beta} b^{\beta}$, η represents the removal ratio of HCB, $\eta = S_{b0}/S_{bi}$. During the degradation experiment, the values of β are approximately 1, so Eq. (18) can be simplified as Eq. (19):

$$1+\eta = -\frac{2v}{S_{bi}\delta I_0^{\alpha}} \tag{19}$$

Based on Eq. (19), the removal ratio can be improved by increasing the initial HCB concentration or the UV light intensity, or by reducing the flow rate. In practical terms, it is obviously not meaningful to improve HCB removal efficiency by enriching its concentration, but it would be suitable methods by increasing UV light intensity or prolonging the reaction time.

3.5. Experimental validation of the model

The experimental data with different initial HCB concentrations and flow, as mentioned above, are shown in Fig. 6. It is clear that 1+η and v are well fit with linear curves and

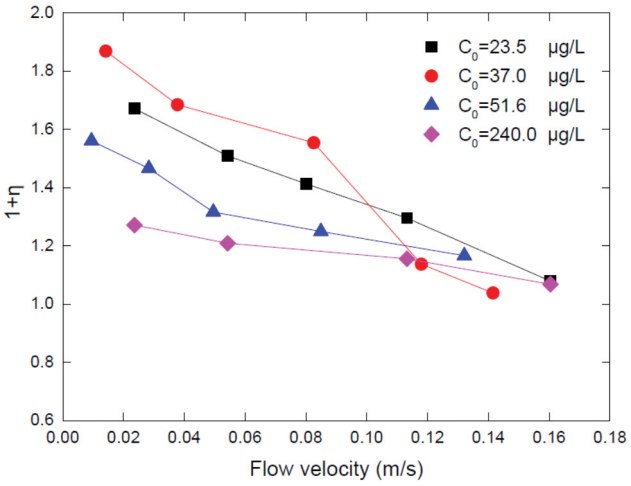

Fig. 6. HCB removal ratio at different initial concentrations under the UV light intensity of 80 μW/cm².

the slope of the lines is $-2/S_{bi}\delta I_0^{\alpha}$. The R^2 are 0.99, 0.96, 0.91 and 0.97 respectively for initial HCB concentrations 23.5, 37.0, 51.6 and 240 μg/L. And the HCB removal ratio will be almost zero at flow velocity around 0.16 m/s, indicating that an appropriate residence reaction time is essential for the removal of HCB in this photoreactor system.

4. Conclusions

A novel photoreactor composed of quartz tubes deposited with a TiO_2 film that is equivalent to a plug flow reactor was employed to effectively and efficiently remove the persistent toxic pollutant—HCB in water. Different operational parameters including initial HCB concentration, flow velocities, UV light intensity, and the existence of organic matter were investigated. It was found that the degradation effect of HCB can be improved in the UV/photocatalytic system at lower flow velocities due to the longer residence time, and higher degradation efficiency occurred at flow velocity around 0.01–0.03 m/s. Furthermore, the degradation efficiency was enhanced remarkably with the increase of UV light intensity linearly, and the highest degradation efficiency was more than 80% under three UV lamps. Besides, the presence of humic acid can result in the enhancement on the removal rate of HCB. Especially, the removal extent was much higher at lower humic acid concentration, which can be ascribed to the photosensitization of the system upon adding suitable humic acid. Finally, a mathematical model was developed in order to establish a kinetic model for the photoreactor. The model was further verified with experimental data, which validated the predictive capability and demonstrated the removal ratio in terms of initial HCB concentration and UV light intensity.

References

[1] L. Reed, V. Buchner, P.B. Tchounwou, Environmental toxicology and health effects associated with dinitrotoluene exposure, Rev. Environ. Health, 22 (2007) 213–244.

[2] Y. Dong, Y. Li, C. Zhao, Y. Feng, S. Chen, Y. Dong, Mechanism of the rapid mechanochemical degradation of hexachlorobenzene with silicon carbide as an additive, J. Hazard. Mater., 379 (2019) 120653, doi: 10.1016/j.jhazmat.2019.05.046.
[3] S.C. Chang, C.W. Yeh, S.K. Lee, T.W. Chen, L.C. Tsai, Efficient remediation of river sediments contaminated by polychlorinated biphenyls and hexachlorobenzene by coupling in situ phase-inversion emulsification and biological reductive dechlorination, Int. Biodeterior. Biodegrad., 140 (2019) 133–143.
[4] V.G. Zuin, F. Airoldi, N.R. Nascimento, M.D. Landgraf, M. Rezende, Determination of pentachlorophenol and hexachlorobenzene in natural waters affected by industrial chemical residues, J. Braz. Chem. Soc., 10 (1999) 25–30.
[5] J. Wang, J.S. Sun, Simultaneous determination of pentachlorophenol and hexachlorobenzene in river sediments, J. Chin. Mass Spectrom. Soc., 27 (2006) 79–83.
[6] J.P. Arrebola, M. Fernandez-Rodriguez, F. Artacho-Cordon, C. Garde, F. Perez-Carrascosa, I. Linares, I. Tovar, B. Gonzalez-Alzaga, J. Exposito, P. Torne, M.F. Fernandez, N. Olea, Associations of persistent organic pollutants in serum and adipose tissue with breast cancer prognostic markers, Sci. Total Environ., 566–567 (2016) 41–49.
[7] L. Hardell, S.O. Andersson, M. Carlberg, L. Bohr, B. van Bavel, G. Lindstrom, H. Bjornfoth, C. Ginman, Adipose tissue concentrations of persistent organic pollutants and the risk of prostate cancer, J. Occup. Environ. Med., 48 (2006) 700–707.
[8] S.G. Jiang, Determination of BHC, DDT, hexachlorobenzene, heptachlor and chlorothalonil in water by GC, China Water Wastewater, 27 (2011) 92–95.
[9] M.I. Badawy, R.A. Wahaab, A.S. El-Kalliny, Fenton-biological treatment processes for the removal of some pharmaceuticals from industrial wastewater, J. Hazard. Mater., 167 (2009) 567–574.
[10] P. Battistoni, E. Cola, F. Fatone, D. Bolzonella, A.L. Eusebi, Micropollutants removal and operating strategies in ultrafiltration membrane systems for municipal wastewater treatment: preliminary results, Ind. Eng. Chem. Res., 46 (2007) 6716–6723.
[11] H.J. Liu, J.H. Qu, R.H. Dai, J. Ru, Z.J. Wang, A biomimetic absorbent for removal of trace level persistent organic pollutants from water, Environ. Pollut., 147 (2007) 337–342.
[12] G. Cravotto, S. Di Carlo, B. Ondruschka, V. Tumiatti, C.M. Roggero, Decontamination of soil containing POPs by the combined action of solid Fenton-like reagents and microwaves, Chemosphere, 69 (2007) 1326–1329.
[13] G. Cravotto, S. Di Carlo, V. Tumiatti, C. Roggero, H.D. Bremner, Degradation of persistent organic pollutants by Fenton's reagent facilitated by microwave or high-intensity ultrasound, Environ. Technol., 26 (2005) 721–724.
[14] Venny, S. Gan, N.K. Ng, Current status and prospects of Fenton oxidation for the decontamination of persistent organic pollutants (POPs) in soils, Chem. Eng. J., 213 (2012) 295–317.
[15] Z. Barbierikova, E. Plizingrova, M. Motlochova, P. Bezdicka, J. Bohacek, D. Dvoranova, M. Mazur, J. Kupcik, J. Jirkovsky, J. Subrt, J. Krysa, V. Brezova, N-Doped titanium dioxide nanosheets: preparation, characterization and UV/visible-light activity, Appl. Catal., B, 232 (2018) 397–408.
[16] S. Kohtani, A. Kawashima, H. Miyabe, Reactivity of trapped and accumulated electrons in titanium dioxide photocatalysis, Catalysts, 7 (2017) 303, doi: 10.3390/catal7100303.
[17] K. Tanaka, K. Harada, S. Murata, Photocatalytic deposition of metal ions onto TiO_2 powder, Sol Energy, 36 (1986) 159–161.
[18] J.G. Mahy, S.D. Lambert, R.G. Tilkin, C. Wolfs, D. Poelman, F. Devred, E.M. Gaigneaux, S. Douven, Ambient temperature ZrO_2-doped TiO_2 crystalline photocatalysts: highly efficient powders and films for water depollution, Mater. Today Energy, 13 (2019) 312–322.
[19] N. Wang, X. Li, Y. Yang, T. Guo, X. Zhuang, S. Ji, T. Zhang, Y. Shang, Z. Zhou, Enhanced photocatalytic degradation of sulfamethazine by Bi-doped TiO_2 nano-composites supported by powdered activated carbon under visible light irradiation, Sep. Purif. Technol., 211 (2019) 673–683.
[20] M. Karches, M. Morstein, P. von Rohr, R.L. Pozzo, J.L. Giombi, M.A. Baltanas, Plasma-CVD-coated glass beads as photocatalyst for water decontamination, Catal. Today, 72 (2002) 267–279.
[21] M.J. Garcia-Martinez, L. Canoira, G. Blazquez, I. Da Riva, R. Alcantara, J.F. Llamas, Continuous photodegradation of naphthalene in water catalyzed by TiO_2 supported on glass Raschig rings, Chem. Eng. J., 110 (2005) 123–128.
[22] B. Tryba, Immobilization of TiO_2 and Fe-C-TiO_2 photocatalysts on the cotton material for application in a flow photocatalytic reactor for decomposition of phenol in water, J. Hazard. Mater., 151 (2008) 623–627.
[23] S.N. Hosseini, S.M. Borghei, M. Vossoughi, N. Taghavinia, Immobilization of TiO_2 on perlite granules for photocatalytic degradation of phenol, Appl. Catal., B, 74 (2007) 53–62.
[24] J.Q. Li, L.P. Li, L. Zheng, Y.Z. Xian, L.T. Jin, Determination of chemical oxygen demand values by a photocatalytic oxidation method using nano-TiO_2 film on quartz, Talanta, 68 (2006) 765–770.
[25] S.Z. Kang, Z.F. Gu, D.Y. Gu, J. Mu, Immobilization and photocatalytic activity of TiO_2 nanoparticles on porous aluminium foil, J. Dispersion Sci. Technol., 26 (2005) 169–171.
[26] Y. Chen, D.D. Dionysiou, Immobilization of transparent NaNo-TiO_2 photocatalytic films on stainless steel for water purification, Abstr. Papers Am. Chem. Soc., 229 (2005) U922.
[27] J.M. Lee, M.S. Kim, B.W. Kim, Photodegradation of bisphenol-A with TiO_2 immobilized on the glass tubes including the UV light lamps, Water Res., 38 (2004) 3605–3613.
[28] K.V.S. Rao, A. Rachel, M. Subrahmanyam, P. Boule, Immobilization of TiO_2 on pumice stone for the photocatalytic degradation of dyes and dye industry pollutants, Appl. Catal., B, 46 (2003) 77–85.
[29] M. Zhang, M. Liu, Y. Jiang, J. Li, Q. Chen, Synthesis of immobilized CdS/TiO_2 nanofiber heterostructure photocatalyst for efficient degradation of toluene, Water Air Soil Pollut., 231 (2020), doi: 10.1007/s11270-020-4461-x.
[30] M. Malakootian, A. Nasiri, M.A. Gharaghani, Photocatalytic degradation of ciprofloxacin antibiotic by TiO_2 nanoparticles immobilized on a glass plate, Chem. Eng. Commun., 207 (2020) 56–72.
[31] J.C. Espindola, R.O. Cristovao, A. Mendes, R.A.R. Boaventura, V.J.P. Vilar, Photocatalytic membrane reactor performance towards oxytetracycline removal from synthetic and real matrices: suspended vs immobilized TiO_2-P25, Chem. Eng. J., 378 (2019) 122114, doi: 10.1016/j.cej.2019.122114.
[32] H. Belayachi, B. Bestani, N. Benderdouche, M. Belhakem, The use of TiO_2 immobilized into grape marc-based activated carbon for RB-5 Azo dye photocatalytic degradation, Arabian J. Chem., 12 (2015) 3018–3027.
[33] S. Sabar, M.A. Nawi, A.H. Jawad, R. Schneider, Enhanced photocatalytic degradation of phenol by immobilized TiO_2/dye-loaded chitosan, Desal. Water Treat., 167 (2019) 190–199.
[34] D.D. Claudio, A.R. Phani, S. Santucci, Enhanced optical properties of sol-gel derived TiO_2 films using microwave irradiation, Opt. Mater., 30 (2007) 279–284.
[35] J.R. Bolton, M.I. Stefan, P.S. Shaw, K.R. Lykke, Determination of the quantum yields of the potassium ferrioxalate and potassium iodide-iodate actinometers and a method for the calibration of radiometer detectors, J. Photochem. Photobiol., A, 222 (2011) 166–169.
[36] W.L. Wang, Q.Y. Wu, Z.M. Li, Y. Lu, Y. Du, T. Wang, N. Huang, H.Y. Hu, Light-emitting diodes as an emerging UV source for UV/chlorine oxidation: carbamazepine degradation and toxicity changes, Chem. Eng. J., 310 (2017) 148–156.
[37] J. Hu, Z. Huang, J. Yu, Highly-effective mechanochemical destruction of hexachloroethane and hexachlorobenzene with Fe/Fe_3O_4 mixture as a novel additive, Sc i. Total Environ., 659 (2019) 578–586.
[38] C. Mauger, R. Volk, N. Machicoane, M. Bourgoin, C. Cottin-Bizonne, C. Ybert, F. Raynal, Diffusiophoresis at the macroscale, Phys. Rev. Fluids, 1 (2016) 363–368.
[39] S. Bendjabeur, R. Zouaghi, B. Zouchoune, T. Sehili, DFT and TD-DFT insights, photolysis and photocatalysis investigation of

three dyes with similar structure under UV irradiation with and without TiO_2 as a catalyst: effect of adsorption, pH and light intensity, Spectrochim. Acta A, 190 (2018) 494–505.
[40] O.M. Alfano, R.J. Brandi, A.E. Cassano, Degradation kinetics of 2,4-D in water employing hydrogen peroxide and UV radiation, Chem. Eng. J., 82 (2001) 209–218.
[41] H.T. Chang, N.M. Wu, F.Q. Zhu, A kinetic model for photocatalytic degradation of organic contaminants in a thin-film TiO_2 catalyst, Water Res., 34 (2000) 407–416.
[42] M.R. Hoffmann, S.T. Martin, W. Choi, D.W. Bahnemann, Environmental applications of semiconductor photocatalysis, Chem. Rev., 95 (1995) 69–96.